Manuscript prepared for Atmos. Chem. Phys.
with version 4.2 of the LaTeX class copernicus.cls.
Date: 9 June 2014

Characterization of OMI tropospheric NO_2 over the Baltic Sea region

I. Ialongo[1], J. Hakkarainen[1], N. Hyttinen[1], J.-P. Jalkanen[2], L. Johansson[2], K. F. Boersma[3,4], N. Krotkov[5], and J. Tamminen[1]

[1]Finnish Meteorological Institute, Earth Observation Unit, Helsinki, Finland
[2]Finnish Meteorological Institute, Air Quality Unit, Helsinki, Finland
[3]Royal Netherlands Meteorological Institute, Climate Observations Department, De Bilt, the Netherlands
[4]Wageningen University, Meteorology and Air Quality group, Wageningen, the Netherlands
[5]Atmospheric Chemistry and Dynamics, NASA Goddard Space Flight Center, Greenbelt, Maryland, USA

Abstract. Satellite-based data are very important for air-quality applications in the Baltic Sea region, because they provide information on air pollution over the sea and where ground-based and aircraft measurements are not available. Both the emissions from urban sites over land and ships over sea, contribute to tropospheric NO_2 levels. Tropospheric NO_2 monitoring at high latitudes using satellite data is challenging because of the reduced light hours in winter and the weak signal due to the low Sun, which make the retrieval complex.

This work presents a characterization of tropospheric NO_2 columns based on case-study analysis in the Baltic Sea region, using the Ozone Monitoring Instrument (OMI) tropospheric NO_2 standard product. Previous works have focused on larger seas and lower latitudes. The results of this paper showed that, despite the regional area of interest, it is possible to distinguish the signal from the main coastal cities and from the ships by averaging the data over a seasonal time range. The summertime NO_2 emission and lifetime values ($E' = (1.5 \pm 0.4)$ mol/s and $\tau = (3 \pm 1)$ h, respectively) in Helsinki were estimated from the decay of the signal with distance from the city centre. These results agree within the uncertainties with the emission from existing database. For comparison, the results for the cities of Saint Petersburg and Stockholm are also shown. The method developed for megacities was successfully applied to smaller-scale sources, in both size and intensity, which is located at high latitudes ($\sim 60^\circ$ N). The same methodology could be applied to similar-scale cities elsewhere, as long as they are relatively isolated from other sources.

Transport by the wind plays an important role in the Baltic Sea region. The NO_2 spatial distribution is mainly determined by the contribution of westerly winds, which dominate the wind patterns during summer. The comparison between the ship emissions from model calculations and OMI NO_2 tropospheric columns supports the applicability of satellite data for ship emission monitoring. In particular, both the ship emission data and the OMI observations showed similar year-to-year variability, with a drop in the year 2009, corresponding to the effect of the financial crisis.

Correspondence to: I. Ialongo (iolanda.ialongo@fmi.fi)

1 Introduction

Nitrogen oxides (NO_x=$NO + NO_2$) play an important role in tropospheric chemistry, participating in ozone and aerosol production processes. NO_x is mainly generated in polluted regions by anthropogenic combustion and it is toxic when present at high concentrations at the surface. An important source of NO_x is also from ship emissions, as they represent a sizeable fraction (3–6 $TgNyr^{-1}$) of the global NO_x production (50 $TgNyr^{-1}$) (Beirle et al., 2004 and references therein). NO_x ship emissions are the most dominant anthropogenic source in the marine atmospheric boundary layer (MBL), far away from densely populated coasts; this is particularly important, since ozone production efficiency is high at the low NO_x concentrations typically occurring in the MBL. The balance between NO and NO_2 depends on the photolysis rate of NO_2.

Satellite-derived tropospheric NO_2 data have been extensively used to monitor air quality over polluted and urban areas (see, e.g., some recent results in Russell et al., 2012; Bechle et al., 2013; David et al., 2013; Ghude et al., 2013; Hilboll et al., 2013; Lamsal et al., 2013). Van der A et al. (2008), for example, estimated the NO_2 trends on global scale using 10 yr of satellite data, identifying the largest increase over eastern China. Furthermore, Castellanos and Boersma (2012) observed a reduction in nitrogen oxides over Europe driven by the 2008–2009 financial recession and by the European NO_x emission regulation. Recently, Streets et al. (2013) presented an overview of the current capability of emissions estimation from satellite retrievals.

The tropospheric NO_2 data from several satellite-based instruments showed also the capability to identify the major shipping lanes in the world. Beirle et al. (2004) presented the first detection of ship tracks in NO_2 maps derived from satellite data using GOME (Global Ozone Monitoring Experiment) data, along the shipping lane from Sri Lanka to Indonesia. Richter et al. (2004), Franke et al. (2009) and Marmer et al. (2009) extended the analysis using combined tropospheric NO_2 data from several satellite instruments. The global economical cycle and satellite-derived NO_2 trends over the major international shipping lanes have been recently compared by de Ruyter de Wildt et al. (2012). Vinken et al. (2014) used the GEOS-Chem model to produce a ship emission inventory based on OMI DOMINO tropospheric NO_2 products, including the Baltic Sea region.

Shipping contributes substantially to air pollution in Europe and the health of coastal populations, and the Baltic Sea ecosystem can be affected by increasing emissions from maritime transportation. Corbett et al. (2007) assessed that the shipping-related emissions are responsible for about 60 000 deaths annually and they estimated that, globally, the annual mortalities due to ship pollution may have increased by 40 % by 2012. In contrast to the NO_x emissions over land, currently there is no specific legislation to limit the NO_x emissions from ships. This produced an increase in shipping emissions estimated by about 3 % per year (Eyring et al., 2010). Furthermore, the Baltic Sea is one of the most intensely trafficked marine areas in the world. According to IMO (2002), there are more than 2000 large vessels at any given time and about 3500–5000 different vessels are in operation in the Baltic Sea region every month. Therefore, there is a strong need for monitoring the NO_x emissions from ships in the Baltic Sea region, together with the land-derived monitoring of emissions. According to European Directives, the so-called SO_x and NO_x Emission Control Areas (SECA and NECA) will be implemented in the Baltic Sea and the need for air-pollution monitoring will further increase. Recently, the authorities postponed the application of the NECA rules until 2021.

Satellite-based tropospheric NO_2 columns from the Dutch-Finnish Ozone Monitoring Instrument (OMI), flying onboard NASA's EOS-Aura satellite, became available in 2004 and provide almost-daily global coverage with nominal spatial resolution of $13 \times 24\,km^2$ at nadir (Boersma et al., 2011; Bucsela et al., 2013). The Baltic Sea and its coastal region, however, are challenging; high-latitude regions may suffer from missing data because the NO_2 observations with high solar-zenith angle or snow/ice surface are not considered reliable and, therefore, excluded from the analysis. The NO_x emissions in the Baltic Sea region are also much lesser than in other more-polluted regions, making signal detection more challenging. Furthermore, being that the Baltic Sea region is relatively small, the contributions from the different sources (land and marine) can be mixed.

Most of the previous studies on monitoring tropospheric NO_2 from satellite focused on middle-low latitudes (see, e.g., Beirle et al., 2011; de Ruyter de Wildt et al., 2012). One exception is the paper by McLinden et al. (2012), who looked at air quality over the Canadian oil sands using satellite data. The uncertainties of NO_x shipping and city emissions as well as estimates of lifetime remain large (see e.g., Stavrakou et al., 2013)), especially for relatively weak sources located at high latitudes. Thus, it is important to study the tropospheric NO_2 pollution in this region.

This paper will focus on monitoring the tropospheric NO_2 levels over the Baltic Sea region, both over marine and coastal areas. In particular, two case studies will be analysed in details: the city of Helsinki and the main shipping lane in central Baltic Sea. The total emission and lifetime will be estimated in Helsinki using OMI NO_2 data and wind information and compared with existing emission informations. The results for Saint Petersburg and Stockholm will be also presented. In addition, the changes in NO_2 levels over the period 2005–2011 will be analysed and compared with the information derived from ship emission modeling.

2 Data and methodology

The OMI NO_2 tropospheric columns were used in this work. Two NO_2 products are available from OMI: NASA's standard product (SP) version 2.1 (Bucsela et al., 2013) and KNMI's DOMINO product version 2 (Boersma et al., 2011). Both products share the same slant column derivation based on the DOAS (Differential Optical Absorption Spectroscopy) method, but differ in a way of converting slant columns into the tropospheric vertical columns. The OMI NO_2 standard product, SP version 2.1 was considered for this study. The algorithm is described in detail by Bucsela et al. (2013), as well as the initial comparison with DOMINO V2 product and aircraft in situ measurements. Comprehensive validation with independent measurements is presented by Lamsal et al. (2014). They show that OMI retrievals are lower in urban regions and higher in remote areas, but generally in agreement with other measurements within $\pm 20\%$.

In this work, the tropospheric NO_2 Level 2 data were gridded on $0.1^\circ \times 0.1^\circ$ in latitude and longitude and averaged over seasonal time scales. Averaging over many days over a grid box smaller than the instrument pixel size, allows an increased effective spatial resolution (Fioletov et al., 2011). The OMI pixels corresponding to SZA larger than 70° and with effective cloud fraction (OMCLDO2 product) larger than 30 % were removed before gridding the data. OMI pixel size ranges between $13 \times 24\,km^2$ in the center of the swath and about $28 \times 150\,km^2$ at the edges. Only the OMI pixel with number from 6 to 24 were included in the analysis to take into account only central small pixels and to avoid the pixels corrupted by the row anomaly. The analysis focused on summer season (1 June–31 August), when more data are available at the latitudes of the Baltic Sea region.

The methodology developed by Beirle et al. (2011) for megacities, was applied to OMI data in the Baltic Sea region, with some differences. The effect of transport by the wind was analysed using the ECMWF wind mean values at 12:00 UTC below 950 hPa altitude with 0.25 degrees resolution. The local time in the area of interest ranges between UTC+1 and UTC+2, which approximately corresponds to the nominal overpass time of OMI (13:45 LT). The daily NO_2 data were gridded taking into account only the pixels where the wind speed (w) is smaller than $5\,\mathrm{ms}^{-1}$ (while a threshold of $2\,\mathrm{ms}^{-1}$ was used in the original method), analysing separately different wind directions (from north, south, east and west), once the weak winds were removed. The wind directions were separated identifying four different sectors (from NW to NE, from NE to SE, from SE to SW and from SW to NW), while eight sectors were identified in Beirle et al. (2011). This allows to improve the sample size, thus increasing the signal-to-noise ratio.

The city of Helsinki is considered to characterize an urban site with low emissions and the central area of the Baltic Sea to evaluate the contribution from ship emissions. The NO_2 emission and lifetime in Helsinki were estimated from the average decay of the signal with the distance from the city centre. Westerly winds were taken into account in the analysis, because the largest part of the data is collected under these conditions. The model proposed by Beirle et al. (2011) was used to fit the NO_2 line densities, which were derived integrating the NO_2 data in across-wind direction over 2 latitude degrees interval. The fitting model M, as a function of the the distance from the city centre x, is described in Equation 1.

$$M(x) = E \cdot e \otimes G + B, \tag{1}$$

where the convolution of the exponential (e) and the Gaussian (G) functions, is scaled by the a factor E and the offset factor B. The downwind exponential function e is

$$e(x) = \exp\left(-\frac{x - X}{x_0}\right), \tag{2}$$

while it is null upwind. X is the location of the source with respect to city centre and x_0 is the e-folding distance (i.e., the distance over which the linear density decreases by a factor of e). The Gaussian function G is defined as

$$G(x) = \frac{1}{\sqrt{2\pi}\sigma} \exp\left(\frac{-x^2}{2\sigma^2}\right), \tag{3}$$

where σ is the Gaussian function width. The parameter x_0 derived from the fit, was then used to calculate the summer mean lifetime $\tau = x_0/w$, where w is the mean zonal wind speed in the direction from west to east. This lifetime must be considered as a dispersion time, which includes the effects of chemical conversion, wind advection and deposition. The coefficient E has to be considered as a burden parameter, which refers to the total amount of molecules observed near the source. The emission parameter $E' = E/\tau$ (in mol/s) was also derived and compared to the emission from EMEP (European Monitoring and Evaluation Programme) database (available at www.ceip.at). The background factor B is also provided. The mathematical notation used here is the same described by Beirle et al. (2011) in the supporting material. The estimation problem is nonlinear with five parameters to be estimated (E, x_0, B, σ and X). The posterior distribution of these unknown parameters was solved using Markov chain Monte Carlo (MCMC) sampling method, which is very useful in low-dimensional non-Gaussian problems allowing also the non-linearity to be properly modelled. Non-informative prior distribution was assumed for all the unknown parameters. For the practical implementation of the algorithm, the MCMC Toolbox by Laine (2008) was used and the adaptive MCMC algorithms by Haario et al. (2001) and Haario et al. (2006) were found to be easily applicable in this case. The convergence of the MCMC algorithm was ensured by sampling a long-enough chain (100 000 points). The estimates of the parameters E, B and e-folding distance x_0 were computed as mean (expectation) values of the posterior distribution and the uncertainty was characterized using the standard deviation of the posterior distribution around the estimate. The same approach is used to derive the emission and lifetime in Saint Petersburg and Stockholm.

The OMI NO_2 tropospheric columns in the MBL were compared with the NO_x emissions of marine traffic as derived from the model STEAM (Ship Traffic Emission Assessment Model), based on the messages provided by the Automatic Identification System (AIS), which enable the positioning of ships with high spatio-temporal resolution (Jalkanen et al., 2009, 2012).

3 Results

3.1 OMI tropospheric NO_2 timeseries

Figure 1 (upper-left panel) shows the map over the Baltic Sea region of OMI NO_2 tropospheric columns averaged over the summer days 2005–2011. The major urban NO_2 sources (marked by their initials and white boxes), i.e., the city of Helsinki (60.2° N, 25.0° E), Saint Petersburg (59.95° N, 30.3° E) and Stockholm (59.3° N, 18.0° E), are visible as red-black spots. In the same panel it is possible to identify the main shipping lane in the Baltic Sea, going from south-west to north-east with a higher signal in the central area of the Baltic Sea. The focus area (Fig. 1 – white rectangle around the point 57.5° N, 19° E) over the Baltic Sea was selected to minimize the influence of the emissions from land sources. Other regions over sea (i.e. Stockholm–Helsinki lane) were not analysed to avoid possible influence of urban sources.

Figure 1 (lower-left panel) shows the summer mean NO_2 map when the wind speed (w), is smaller than $5\,\mathrm{ms}^{-1}$. The NO_2 values corresponding to the pixels with stronger

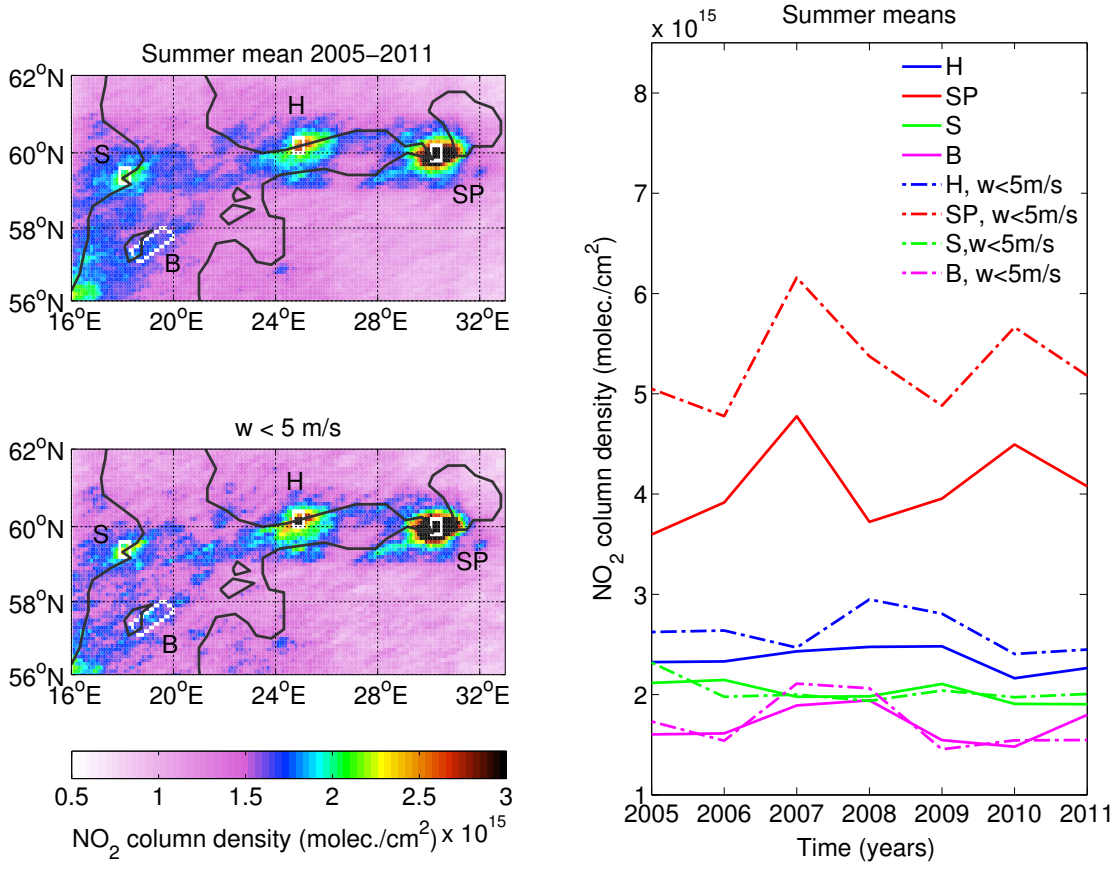

Fig. 1. OMI tropospheric NO_2 column averaged over the summer days in 2005–2011, under all wind and weak wind conditions (upper and lower-left panel, respectively). The main coastal cities and the selected area in the Baltic Sea region are marked with their initials: Helsinki (H, 60.2° N, 25.0° E), Stockholm (S, 59.3° N, 18.0° E), Saint Petersburg (SP, 59.95° N, 30.3° E) and the Baltic Sea (B, 57.5° N, 19° E). The right panel illustrates the time series of the seasonal means of NO_2 for these locations. The grid pixels included in the summer means are marked by the white boxes in the left panels.

wind speed were removed in order to highlight the emission sources. In this case, the high NO_2 signal is stronger and it remains closer to the sources; the number of data used in the average is smaller than in the previous case (about 30 % of the total available data). The wind intensity and direction play an important role in determining the tropospheric NO_2 distribution and they will be analysed later in this work. Other features visible from Fig. 1 are the cities of Tallinn (59.4° N, 24.7° E) and Turku (60.45° N, 22.3° E).

In Fig. 1 (right panel), the 2005–2011 time series of the summer means over the main cities and over the Baltic Sea region, are shown under all wind conditions (continuous lines) as well as when strong winds were removed (dashed lines). The analysis was restricted to the summer months since not enough and homogeneously distributed data were available during other seasons. The time series show a local minimum in 2009 in Saint Petersburg and in the Baltic Sea region. A similar local minimum of NO_2 in 2009 was observed by Castellanos and Boersma (2012) for several cities in Europe and by de Ruyter de Wildt et al. (2012) for the major shipping lanes. In both cases, the observed reduction was interpreted as the consequence of the 2008–2009 financial recession, which caused a reduction of the emissions from both urban and ship sources. This behaviour is more apparent under weak-wind conditions (dashed lines in Fig. 1); the transport by the wind acts to dampen the year-to-year variability in NO_2 tropospheric columns. Helsinki and Stockholm time series remain more flat during the considered period. In particular, a NO_2 decrease from year 2008 to 2009 was observed in Helsinki, but the minimum NO_2 value was observed in 2010, in agreement with previous results (see inset city names in Fig. 6 in Castellanos and Boersma, 2012). Thus, other factors than the anthropogenic sources may have contributed to the NO_2 distribution over Helsinki. Overall, the absolute levels of tropospheric NO_2 are higher for the urban sites (especially Saint Petersburg) and smaller for the central Baltic Sea. One must note that the largest ship activity in the Baltic Sea is observed during summer (Jalkanen et al.,

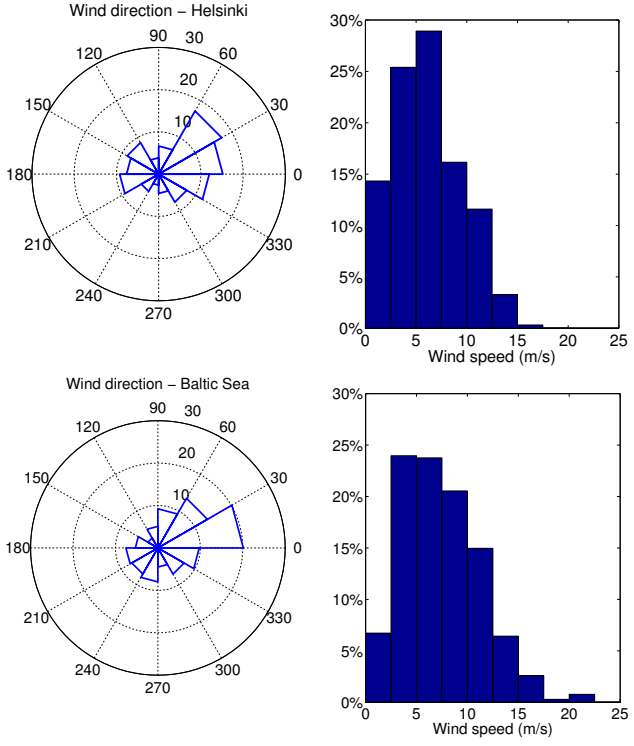

Fig. 2. Wind directions (left panels) and wind-speed histogram (right panels) averaged below 950 hPa level over all summers 2005–2011. The azimuthal angle 0 corresponds to wind from west to east (according to the ECMWF definition). Both the data from Helsinki and the central Baltic Sea area, as defined by the white boxes in Fig. 1, are presented in the upper and lower panels, respectively.

2013), because of the high season of passenger traffic. On the other hand, the pollution in the cities is generally smaller during summer than in other seasons. Thus, the tropospheric NO_2 columns over the shipping lane might be relatively large compared to the signal over the urban sites.

3.2 Helsinki case study

First, the distribution of wind intensity and direction in Helsinki were analysed. Figure 2 (upper panel) shows the distribution of the wind directions as a polar plot, together with the histogram of the wind speed at 12:00 (UTC time) during summer 2005–2011 over Helsinki (corresponding to the pixels in the white boxes of Fig. 1). The polar plots show that the wind patterns are generally dominated by westerlies during summer. The histograms follow a log-normal distribution with peak between 5 and 7.5 ms^{-1}. The fraction of pixels with wind speed below the threshold of 5 ms^{-1} is below 35 %. This percentage was calculated with respect to the total number of pixels included in the area marked by the white boxes (Fig. 1). This means that the largest part of the pixels is removed when only the weak winds are taken into account, introducing a larger statistical error in the calculation of the mean NO_2 spatial distribution.

Figure 3 illustrates the effect of the different wind directions and speeds on the tropospheric NO_2 distribution around Helsinki area. The central panel in Fig. 3 refers to the pixels where only weak winds were considered ($w < 5\,\mathrm{ms}^{-1}$); the four surrounding panels correspond to the NO_2 tropospheric columns averaged separately for different wind directions (winds blowing from north, west, south and east, are respectively showed moving clockwise from the top panel). Each grid pixel is associated with one of the wind sectors according to the corresponding ECMWF average wind direction below 950 hPa. The resulting NO_2 spatial patterns clearly show the outflow of NO_2 from Helsinki, consistently with the wind directions, so that when wind blows, for example, from west, the largest NO_2 signal is observed east from the city. Similar results were achieved around the city of Riyadh and other megacities as shown by Beirle et al. (2011). The results shown in Fig. 3 demonstrate that the same methodology can be applied to Helsinki and its surrounding capital region, which together have about 1 million inhabitants.

Figure 4 shows the NO_2 line densities (blue colour), sampled using OMI pixels under westerly wind conditions, as a function of the eastward distance to Helsinki. The profile peak is displaced eastward because of the effect of the airmass transport by the westerly winds. The resulting values for e-folding distance $x_0 = (52 \pm 9)$km, the background parameter $B = (3.54 \pm 0.02) \times 10^{22}$ molec./cm and the burden parameter $E = (1.0 \pm 0.1) \times 10^{28}$ molec. were derived from the mean fitted model (Fig. 4 – black line). The summer mean lifetime value $\tau = (3 \pm 1)$h was then estimated by the ratio x_0/w, with $w = (4.9 \pm 0.2)\,\mathrm{m\ s}^{-1}$. The emission was also calculated as $E' = E/\tau = (1.5 \pm 0.4)\,\mathrm{mol\ s}^{-1}$. The emission parameter E' was then compared with EMEP NO_x emission (given as NO_2), $E'_{emep} = (1.8 \pm 0.3)\,\mathrm{mol\ s}^{-1}$ for the period 2007–2011 around Helsinki area, showing agreement within the uncertainties. The yearly emissions from the EMEP database are given with uncertainty up to 15 %.

It must be noted that the emission and lifetime derived from OMI data refer to clear-sky conditions. When only clear-sky pixels are considered (Geddes et al., 2012), a negative bias is expected, mostly because of the accelerated photochemistry, so that both the emission E' and the lifetime would be smaller than for cloudy conditions. This negative bias could be partially compensated by the effect of emission changes in the AMF (Air Mass Factor) calculation. According to NCEP database, the NO_x emissions in Finland, for example, decreased from the late 1990s (when the a-priori information used in OMI algorithm are derived) by about 20 %. Higher emission in the a priori information leads to lower AMFs, resulting in higher tropospheric columns. (Vinken et al., 2014) found that in Europe about 30 % lower emissions produce on average 10 % lower tropospheric columns. In our case, the calculated emission factor for Helsinki might

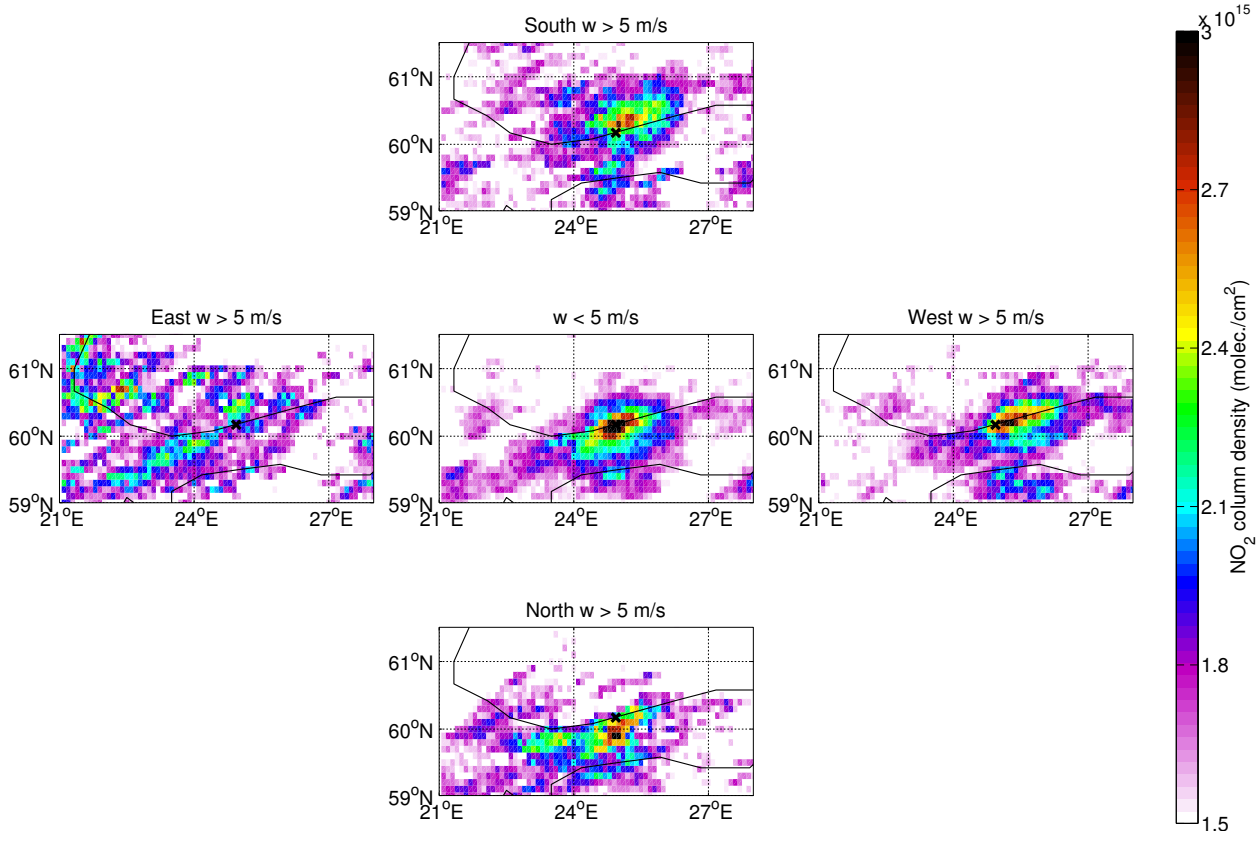

Fig. 3. Summer 2005–2011 mean tropospheric NO_2 columns around Helsinki (black cross) for different wind conditions, i.e., weak wind (central panel) and four main wind direction sectors (surrounding panels). NO_2 maps for winds blowing from north, west, south and east, are respectively shown moving clockwise from the top panel.

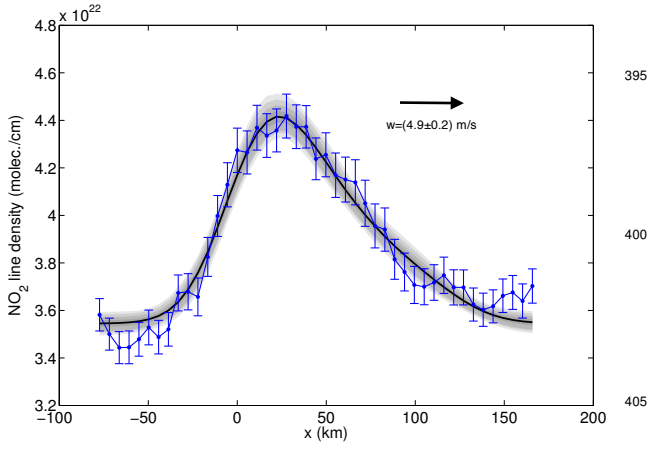

Fig. 4. OMI NO_2 line density (blue colour) for westerly wind conditions as a function of the distance (x) to/from Helsinki. Positive numbers in the x-axis are eastward from the city center. The error bars were derived using the error propagation for the discrete integral. The black line shows the MCMC fitted model and the grey areas correspond to the 50–99 % probability uncertainty regions.

be positively biased.

Despites this effects, the emission E' derived from OMI data agrees within the uncertainties with EMEP emission E'_{emep}. Furthermore, it must be noted that in this work a daytime NO_2 lifetime is derived. This instantaneous lifetime holds for OMI overpass times and is usually shorter than the 24 h-average NO_2 lifetime (see, e.g., Boersma et al., 2008). The lifetime τ agrees within the error bars (but smaller as absolute value) with the summertime value obtained by Beirle et al. (2011) for Moscow ($\tau \simeq (4 \pm 2)$h), which is located at about 5 latitude degrees south of Helsinki.

The errors on the estimated parameters are the standard deviations derived from the MCMC calculations. The error bars in Fig. 4 were calculated using the error propagation for the discrete integral and include the contribution from the statistical error on the mean NO_2 field. The uncertainties on the emission and lifetime depend also on the error associated with OMI tropospheric NO_2 column density (about 30 %, Bucsela et al. (2013)). The wind field patterns also affect the NO_2 spatial distribution and, thus, the parameter calculation. Beirle et al. (2011) introduced an uncertainty of 30 % due to the wind fields. This is similar to the variability in the NO_2 patterns obtained in Helsinki using the wind fields

Table 1. Results of the emission and lifetime (second and third column, respectively) calculation for Helsinki, Saint Petersburg and Stockholm with their total uncertainties. The emission data from the EMEP database are shown for comparison (last column).

City	Emission E' [mol/s]	Lifetime τ [h]	EMEP Emission E'_{EMEP} [mol/s]
Helsinki	1.5±0.4	3.0±1.0	1.8±0.3
Saint Petersburg	5.0±2.0	3.0±1.3	3.0±0.5
Stockholm	2.2±1.1	3.5±1.5	1.4±0.3

at different altitudes instead of the average below 950 hPa. An additional uncertainty comes from the selection of the integration and the fitting intervals. In the Helsinki case, these intervals were selected to avoid the effect of high NO_2 signal from the surrounding emission sources. Applying the error propagation rules, the total uncertainty on E' and τ is larger than 40 %.

The emission and lifetime were similarly calculated for Stockholm and St. Petersburg. The results are summarized in Table 1. The figures corresponding to Fig. 3 and Fig. 4 are shown in the supplementary materials (Fig. S1 and S2, respectively). The wind regimes were similar to Helsinki, with the wind patterns dominated by the westerlies. In both cases the uncertainties on the parameter estimates are larger than in Helsinki because of the larger sensitivity to the selection of the integration range for the linear density calculation. In particular, the effect of other point sources close to the city and the not-perfect symmetry under calm conditions affected the quality of the fit and increased the uncertainty of the results. Despites these limitations, the lifetime values are consistent with the Helsinki case and the emissions are larger in Saint Petersburg than in Helsinki and Stockholm, as expected. Also, the estimated emissions agree within the uncertainties with the EMEP database information (last column in Table 1).

3.3 Baltic Sea shipping case study

The wind intensity and direction were analysed also in the central Baltic Sea area. Figure 2 (lower panel) shows the polar plot of the wind directions and the distribution of the wind speed at noon (UTC time) during summer 2005–2011. The wind distribution is similar to Helsinki as it is generally dominated by the westerlies and the wind-speed histogram peaks between 5 and 7.5 ms^{-1}. The fraction of pixels with wind speed below the threshold of 5 ms^{-1} is about 25 %. The wind effect on NO_2 patterns was analysed in the centre of the Baltic Sea, in the white-dotted area (Fig. 1, left side) where a large NO_2 signal was observed. In this case, the wind conditions are not the only cause of transport of the polluted air, since also the ships, which constitute the main emission source in this region, are moving along the major shipping lane from Denmark to the Gulf of Finland and to Stockholm. The analysis of the number of pixels associated with the different wind directions (not plotted here) confirms that the wind patterns in the Baltic Sea are dominated by westerlies, which give the largest contribution to the mean seasonal NO_2 spatial patterns.

Figure 5 shows the summer average of NO_2 over the Baltic Sea region when all wind conditions (left panel), weak winds (central panel) and westerly winds only (right panel) are taken into account. The high NO_2 signal in the central Baltic Sea area is visible when all wind conditions (left panel) are considered. The signal is also visible when only the weak winds (central panel) are taken into account, even though a smaller amount of data are available under these wind conditions. Surprisingly, when only the westerly winds are considered, the NO_2 signal is stronger than under calm wind conditions. This can be explained by the fact that a larger number of pixels satisfy the wind-driven condition, thus increasing the signal-to-noise ratio. Furthermore, because the shipping lane is directed in SW-NE direction, the emission produced from any point along the shipping lane might be transported along the same lane (and so still contribute to the enhanced NO_2 signal) by the winds from Southwest, which is one of the dominant wind directions (Fig. 2 - lower panel). On the other hand, under strong wind conditions the NO_2 patterns over sea can be influenced by the air masses transported from land sources. For example, the red spot in the lower left corner in Fig. 5 (right panel) is most probably caused by the outflow from southern Sweden and Denmark. In order to reduce the effect of this outflow, the time series analysis was performed under calm wind conditions and limited to the central area of the Baltic Sea (the black box in Fig. 6 centred at 57.5° N–19° E), where the minimum mixing between the emissions from land and sea sources is expected.

The seasonal NO_x emissions (Fig. 6 – left panel) from maritime traffic as derived from STEAM were compared with tropospheric NO_2 columns (Fig. 6 – central panel) for the period July–August 2006–2011. The analysis was restricted to July and August because of a significant data gap in the NO_x emission data in June 2006 and 2010. No NO_x emission information were available for year 2005. The NO_x emission data (Fig. 6 – left panel) show that the ship-emission sources are mostly located along one main shipping lane along the direction from SW to NE, with some secondary branches. The emission patterns correspond to high NO_2 signal observed from OMI data in the central Baltic Sea area (Fig. 6 – central panel).

The time series of both NO_x emissions and OMI NO_2 tro-

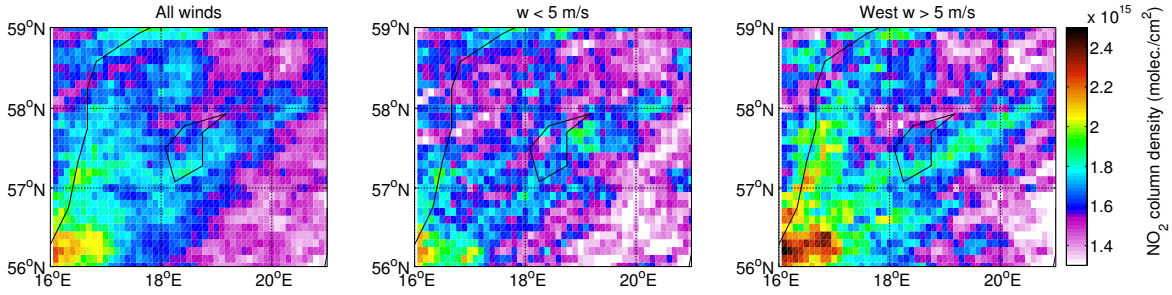

Fig. 5. Summer 2005–2011 mean tropospheric NO_2 columns in the Baltic Sea for all wind conditions (first panel), weak winds, i.e. $w < 5\,\mathrm{m\,s^{-1}}$ (central panel) and westerly winds with $w > 5\,\mathrm{m\,s^{-1}}$ (right panel).

pospheric columns are shown in the right panel in Fig. 6. The areas including the signal peaks in the central Baltic Sea (black boxes in Fig. 6) were selected from both OMI and STEAM datasets, in order to analyse the temporal evolution. Because the emissions and the OMI data do not exactly match in their spatial patterns and because of the different gridding and resolution, the selected boxes do not perfectly coincides.

The time series follow a similar behaviour, both showing an increase up to 2008 and a decrease in 2009, before slightly increasing again until 2011. The tropospheric NO_2 observed from OMI decreased by about 6×10^{14} molec. $\mathrm{cm^{-2}}$ from 2008 to 2009, corresponding to a reduction in the NO_x emissions by about 1.2×10^5 g/month per pixel unit. Thus, the NO_2 relative change is larger by a factor of 2 than the change in the ship emissions. Vinken et al. (2014) derived the ratio β between the changes in NO_x emissions to the changes in NO_2 tropospheric columns in the Baltic Sea, North Sea and other shipping lanes from model calculations. They also found that over the shipping lanes the emission changes lead to substantial changes in NO_2 columns (e.g.. β=0.25 in the Baltic Sea and β=0.58 in the North Sea), up to 2-to-4 times larger than the emission changes.

These results must be analysed considering that the changes in NO_2 tropospheric columns are close to the detection limit for OMI ($\pm 5 \times 10^{14}$ molec. $\mathrm{cm^{-2}}$). Furthermore, the uncertainties related to the calculations from STEAM depend on both the emission factor and the power level of every single ship. When comparing the model results with the existing emission inventories, the difference is of the order of 10–15 % (Jalkanen et al., 2012). In addition, STEAM data might underestimate the ship emissions because of the effect of the small ships, which are not regularly provided with an AIS system (Jalkanen et al., 2013).

4 Summary and discussion

In this paper, the OMI NO_2 tropospheric columns were used to describe air-pollution levels in the Baltic Sea and its coastal area. Both land (urban sites) and marine (ships) case studies were taken into account in the analysis. OMI NO_2 data demonstrated their applicability to detect the signal coming from relatively small emission sources, such as ships and coastal cities at high latitudes. This is the first time ship and urban emissions have been mapped from space with such detail in this area.

The transport of air masses by the wind plays an important role in defining the spatial distribution of NO_2 in the Baltic Sea area, as demonstrated when the NO_2 data were averaged separately for different wind directions. Reducing the analysis to weak-wind conditions ($w < 5\,\mathrm{m\,s^{-1}}$) helps in identifying the urban sources, but it reduces by about 70 % the total number of data available for the seasonal average. When looking at the marine area in the central Baltic Sea, where the ships are the main source of NO_x emission, the NO_2 data corresponding to westerly wind conditions give the largest contribution to the NO_2 spatial patterns. This case corresponds to the situation with the largest continental outflow. On the other hand, the weak winds correspond to the 25 % of the available data in the same marine area.

The analysis of the wind effect on the NO_2 spatial distribution around Helsinki allowed the estimation of the emission coefficient and lifetime. The comparison with EMEP emission information showed good agreement. The method developed for megacities demonstrated applicability also to Helsinki and its surrounding capital region (about 1 million inhabitants). Thus, in principle, the same methodology could be applied to similar small-scale cities elsewhere as long as isolated. The same method was applied to Saint Petersburg and Stockholm obtaining consistent results but larger uncertainties. Furthermore, it can be noted that sorting the data according to the wind speed and direction is a very useful tool for many different applications of satellite data.

The agreement with the ship NO_x emission data from STEAM model confirmed that OMI NO_2 data can be used to detect the signal coming from the ship emissions in a busy area like the Baltic Sea, where the effect of coastal pollution sources can mix with the emission coming from the ships to the marine boundary layer. OMI NO_2 tropospheric columns reproduce the same year-to-year variability of the emissions.

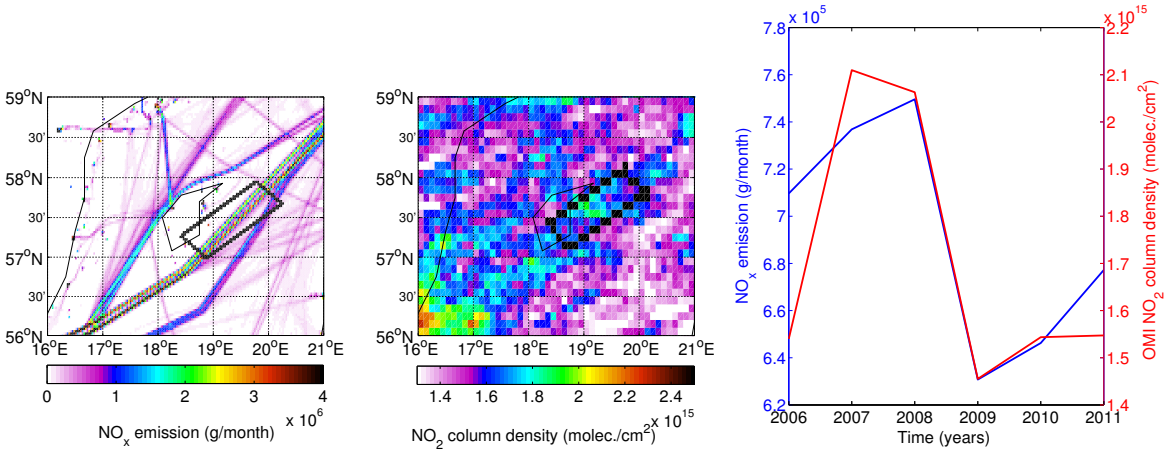

Fig. 6. Comparison between STEAM NO_x emissions and OMI NO_2 tropospheric columns during the period 2006–2011. Left panel: July–August cumulative NO_x emissions from STEAM; central panel: July–August mean NO_2 tropospheric columns from OMI; right panel: time series of both NO_x emissions (blue line) and NO_2 columns (red line) as derived from the mean value within the black boxes in the left and central panel, respectively. Note that the axes have been selected so that the observed decreases have the same size in the plot.

In particular, both the emission data and the OMI observations showed the drop in year 2009, corresponding to the financial crisis. This confirmed the results obtained for other regions (e.g., de Ruyter de Wildt et al., 2012).

This paper demonstrated that satellite data contribute substantially to monitoring pollution levels and environmental changes at high latitude and over the sea, where atmospheric concentration information are sparsely available from other sources. Monitoring the NO_2 levels from satellite in the Baltic Sea region remains challenging for many reasons: the interested area is in darkness for much of the year (and especially cloudy in autumn/winter). Using for example Sun-synchronous satellite, as done in this work, and allowing only a solar-zenith angle smaller than 70° to reduce the uncertainties, means that no data are available from November to February over northern Europe. This highlights the need to develop satellite-based instruments with particular focus on the Arctic region, in order to monitor both land and marine air quality at high latitudes, i.e. with several satellite overpass in one day. In this sense, the NO_2 retrieval should be improved and optimized for situations with high solar-zenith angle and high albedo (as for snow/ice covered surfaces).

Furthermore, the signals coming from ships and from the Baltic Sea coastal areas are relatively small compared to other more polluted regions. This makes the detection even more difficult, because the signal is close to the instrument's detection limit. In addition, the Baltic Sea region is relatively small and the sources of emission are close to each other; this increases the difficulty in identifying the signal coming from different sources. Nevertheless, the method applied in this study allows one to distinguish relatively close and small sources, averaging for many days over a grid box smaller than the instrument pixel size, increasing the effective spatial resolution.

The results achieved in this work might be improved using data with higher spatial resolution, i.e. smaller pixel size, as they will become available in 2016 from TROPOspheric Monitoring Instrument (TROPOMI), within the ESA/GMES Sentinel 5 Precursor mission. The instrument will provide daily global coverage with a high spatial resolution of $7 \times 7\,\mathrm{km}^2$, which will improve the OMI pixel size ($13 \times 24\,\mathrm{km}^2$ at nadir).

Acknowledgements. This work was founded by ESA-SAMBA project on ship emission monitoring in the Baltic Sea area. The Dutch-Finnish-built OMI instrument is part of the NASA EOS Aura satellite payload. The OMI project is managed by KNMI and the Netherlands Agency for Aerospace Programs (NIVR).We acknowledge the NASA Earth Science Division for funding of OMI NO_2 standard product development and archiving. A version of the manuscript was checked for language glitches by Curtis Wood (FMI).

References

Beirle, S., Platt, U., von Glasow, R., Wenig, M., and Wagner, T.: Estimate of nitrogen oxide emissions from shipping by satellite remote sensing, Geophys. Res. Lett., 31, L18102, 10.1029/2004GL020312, 2004.

Beirle, S., Boersma, K. F., Platt, U., Lawrence, M. G., and Wagner, T.: Megacity emissions and lifetimes of nitrogen oxides probed from space, Science, 333, 1737–1739, 10.1126/science.1207824, 2011.

Bechle, M. J., Millet, D. B., and Marshall, J. D.: Remote sensing of exposure to NO_2: satellite versus ground-based measurement in a large urban area, Atmos. Environ., 69, 345–353, 10.1016/j.atmosenv.2012.11.046, 2013.

Boersma, K. F., Jacob, D. J., Eskes, H. J., Pinder, R. W., Wang, J. and van der A, R. J.: Intercomparison of SCIAMACHY and OMI tropospheric NO2 columns: observing the diurnal evolution

of chemistry and emissions from space, J. Geophys. Res., 113, D16S26, 10.1029/2007JD008816, 2008.

Boersma, K. F., Eskes, H. J., Dirksen, R. J., van der A, R. J., Veefkind, J. P., Stammes, P., Huijnen, V., Kleipool, Q. L., Sneep, M., Claas, J., Leitão, J., Richter, A., Zhou, Y., and Brunner, D.: An improved tropospheric NO_2 column retrieval algorithm for the Ozone Monitoring Instrument, Atmos. Meas. Tech., 4, 1905–1928, 10.5194/amt-4-1905-2011, 2011.

Bucsela, E. J., Krotkov, N. A., Celarier, E. A., Lamsal, L. N., Swartz, W. H., Bhartia, P. K., Boersma, K. F., Veefkind, J. P., Gleason, J. F., and Pickering, K. E.: A new stratospheric and tropospheric NO_2 retrieval algorithm for nadir-viewing satellite instruments: applications to OMI, Atmos. Meas. Tech., 6, 2607–2626, 10.5194/amt-6-2607-2013, 2013.

Castellanos, P., and Boersma, K. F.: Reductions in nitrogen oxides over Europe driven by environmental policy and economic recession, Sci. Rep., 2, 265; 10.1038/srep00265, 2012.

Corbett, J. J., Winebrake, J. J., Green, E. H., Kasibhatla, P., Eyring, V., and Lauer, A.: Mortality from ship emissions: a global assessment, Environ. Sci. Technol., 41, 8512–8518, 2007.

David, L. M. and Nair, P. R.: Tropospheric column O_3 and NO_2 over the Indian region observed by Ozone Monitoring Instrument (OMI): seasonal changes and long-term trends, Atmos. Environ., 65, 25–39, 10.1016/j.atmosenv.2012.09.033, 2013.

de Ruyter de Wildt, M., Eskes, H., and Boersma, K. F.: The global economic cycle and satellite-derived NO_2 trends over shipping lanes, Geophys. Res., Lett., 39, L01802, 10.1029/2011GL049541, 2012.

Eyring, V., Isaksen, I. S. A., Berntsen, T., Collins, W. J., Corbett, J. J., Endresen, O., Grainger, R. G., Moldanova, J., Schlager, H., and Stevenson, D. S.: Transport impacts on atmosphere and climate: shipping, Atmos. Environ., 44, 4735–4771, 10.1016/j.atmosenv.2009.04.059, 2010.

Fioletov, V. E., McLinden, C. A., Krotkov, N., Moran, M. D., and Yang, K.: Estimation of SO_2 emissions using OMI retrievals, Geophys. Res. Lett., 38, L21811, 10.1029/2011GL049402, 2011.

Franke, K., Richter, A., Bovensmann, H., Eyring, V., Jockel, P., Hoor, P., and Burrows, J. P.: Ship emitted NO_2 Franke, K., Richter, A., Bovensmann, H., Eyring, V., Jöckel, P., Hoor, P., and Burrows, J. P.: Ship emitted NO_2 in the Indian Ocean: comparison of model results with satellite data, Atmos. Chem. Phys., 9, 7289–7301, 10.5194/acp-9-7289-2009, 2009.

Geddes, J.A., Murphy, J.G., Celarier, E.A., and O'Brien, J.: Biases in long-term NO_2 averages inferred from satellite observations due to cloud selection criteria, Rem. Sens. Environ., 124, 210-216, 2012.

Ghude, S. D., Kulkarni, S. H., Jena, C., Pfister, G. G., Beig, G., Fadnavis, S., and van der A, R. J.: Application of satellite observations for identifying regions of dominant sources of nitrogen oxides over the Indian Subcontinent, J. Geophys. Res., 118, 1075–1089, 10.1029/2012JD017811, 2013.

Haario, H., Saksman, E., and Tamminen, J.: An adaptive Metropolis algorithm, Bernoulli, 7, 223–242, 2001.

Haario, H., Laine, M., Mira, A., and Saksman, E.: DRAM: Efficient adaptive MCMC, Stat. Comput., 16, 339–354, 2006.

Hilboll, A., Richter, A., and Burrows, J. P.: Long-term changes of tropospheric NO_2 over megacities derived from multiple satellite instruments, Atmos. Chem. Phys., 13, 4145–4169, 10.5194/acp-13-4145-2013, 2013.

International Maritime Organization: Safety Of Life At Sea (SOLAS) agreement, regulation 19, Chapter V, 1974, 2002 Amendments.

Jalkanen, J.-P., Brink, A., Kalli, J., Pettersson, H., Kukkonen, J., and Stipa, T.: A modelling system for the exhaust emissions of marine traffic and its application in the Baltic Sea area, Atmos. Chem. Phys., 9, 9209–9223, 10.5194/acp-9-9209-2009, 2009.

Jalkanen, J.-P., Johansson, L., Kukkonen, J., Brink, A., Kalli, J., and Stipa, T.: Extension of an assessment model of ship traffic exhaust emissions for particulate matter and carbon monoxide, Atmos. Chem. Phys., 12, 2641–2659, 10.5194/acp-12-2641-2012, 2012.

Jalkanen, J.-P., Johansson, L., and Kukkonen, J.: A comprehensive inventory of the ship traffic exhaust emissions in the Baltic Sea from 2006 to 2009, Ambio, http://dx.doi.org/10.1007/s13280-013-0389-3,10.1007/s13280-013-0389-3, 2013.

Laine, M.: Adaptive MCMC Methods with Applications in Environmental and Geophysical Models, Finnish Meteorological Institute Contributions, No. 69, available at: http://urn.fi/URN:ISBN:978-951-697-662-7 (last access: 22 January 2014), 2008.

Lamsal, L. N., Martin, R. V., Parrish, D. D., and Krotkov, N. A.: Scaling relationship for NO_2 pollution and urban population size: a satellite perspective, Environ. Sci. Technol., 47, 7855–7861, 10.1021/es400744g, 2013.

Lamsal, L. N., Krotkov, N. A., Celarier, E. A., Swartz, W. H., Pickering, K. E., Bucsela, E. J., Martin, R. V., Philip, S., Irie, H., Cede, A., Herman, J., Weinheimer, A., Szykman, J. J., and Knepp, T. N.: Evaluation of OMI operational standard NO_2 column retrievals using in situ and surface-based NO_2 observations, Atmos. Chem. Phys. Discuss., 14, 14519-14573, doi:10.5194/acpd-14-14519-2014, 2014.

Marmer, E., Dentener, F., Aardenne, J. v., Cavalli, F., Vignati, E., Velchev, K., Hjorth, J., Boersma, F., Vinken, G., Mihalopoulos, N., and Raes, F.: What can we learn about ship emission inventories from measurements of air pollutants over the Mediterranean Sea?, Atmos. Chem. Phys., 9, 6815–6831, 10.5194/acp-9-6815-2009, 2009.

McLinden, C. A., Fioletov, V., Boersma, K. F., Krotkov, N., Sioris, C. E., Veefkind, J. P., and Yang, K.: Air quality over the Canadian oil sands: A first assessment using satellite observations, Geophys. Res. Lett., 39, L04804, 10.1029/2011GL050273, 2012.

Richter, A., Eyring, V., Burrows, J., Bovensmann, H., Lauer, A., Sierk, B., and Crutzen, P.: Satellite measurements of NO_2 from international shipping emissions, Geophys. Res. Lett., 31, L23110, 10.1029/2004GL020822, 2004.

Russell, A. R., Valin, L. C., and Cohen, R. C.: Trends in OMI NO_2 observations over the United States: effects of emission control technology and the economic recession, Atmos. Chem. Phys., 12, 12197–12209, 10.5194/acp-12-12197-2012, 2012.

Stavrakou, T., Müller, J.-F., Boersma, K. F., van der A, R. J., Kurokawa, J., Ohara, T., and Zhang, Q.: Key chemical NO_x sink uncertainties and how they influence top-down emissions of nitrogen oxides, Atmos. Chem. Phys., 13, 9057–9082, 10.5194/acp-13-9057-2013, 2013.

Streets, D. G., Canty, T., Carmichael, G. R., de Foy, B., Dickerson, R. R., Duncan, B. N., Edwards, D. P., Haynes, J. A.,

Henze, D. K., Houyoux, M. R., Jacob, D. J., Krotkov, N. A., Lamsal, L. N., Liu, Y., Lu, Z., Martin, R. V., Pfister, G. G., Pinder, R. W., Salawitch, R. J., and Wecht, K. J.: Emissions estimation from satellite retrievals: a review of current capability, Atmos. Environ., 77, 1011–1042, 2013.

van der A, R. J., Eskes, H. J., Boersma, K. F., van Noije, T. P. C., Van Roozendael, M., DeSmedt, I., Peters, D. H. M. U., and Meijer, E. W.: Trends, seasonal variability and dominant NO_x source derived from a ten year record of NO_2 measured from space, J. Geophys. Res., 113, D04302, 10.1029/2007JD009021, 2008.

Vinken, G. C. M., Boersma, K. F., van Donkelaar, A., and Zhang, L.: Constraints on ship NO_x emissions in Europe using GEOS-Chem and OMI satellite NO_2 observations, Atmos. Chem. Phys., 14, 1353–1369, 10.5194/acp-14-1353-2014, 2014.